Available online at www.sciencedirect.com
SCIENCE DIRECT
Catalysis Today 107–108 (2005) 643–650
CATALYSIS TODAY
www.elsevier.com/locate/cattod

Role of Sn in Pt–Re–Sn/Al_2O_3–Cl catalysts for naphtha reforming

Vanina A. Mazzieri, Javier M. Grau, Carlos R. Vera, Juan C. Yori, José M. Parera, Carlos L. Pieck *

Instituto de Investigaciones en Catálisis y Petroquímica, INCAPE (FIQ-UNL, CONICET), Santiago del Estero 2654, 3000 Santa Fe, Argentina

Available online 15 August 2005

Abstract

The influence of Sn addition on the catalytic activity of Pt–Re/Al_2O_3 naphtha reforming catalysts was studied. Trimetallic Pt–Re–Sn catalysts supported on chlorided alumina were prepared by coimpregnation. The content of Re and Pt was 0.3%, while the Sn load was varied between 0.0 and 0.9% (weight basis). In order to make a comparison, Pt/Al_2O_3 and Pt–Re/Al_2O_3 catalysts were also prepared. The acid function of the catalysts was studied by means of temperature programmed desorption of pyridine and the reaction test of *n*-pentane isomerization. Temperature programmed reduction and cyclohexane dehydrogenation were used to characterize the activity of the metal function. *n*-C_7 dehydrocyclization was used as a test of the combined action of the acid and metal function. It was found that Sn decreases the amount of strong acid sites of chlorided alumina producing catalysts with lower cracking activity. In the case of the trimetallic Pt–Re–Sn catalyst, Sn addition to Pt–Re decreases the hydrogenolytic activity and increases both the isomerization activity and the stability. The best catalyst is the one with 0.1% Sn. The addition of Sn to Pt–Re catalysts also decreases the benzene/*i*-C_7 ratio of the reformate, an important issue from an environmental point of view.

Keywords: Naphtha reforming; Trimetallic catalysts; Pt–Re–Sn

1. Introduction

The catalytic reforming process has the main objective of transforming virgin naphtha cuts of low octane number into gasolines with high octane number. The total amount of aromatic hydrocarbons and branched paraffins is increased. Other than fuel compounds for the gasoline pool, some reformate products are also used as intermediates for the petrochemical industry, as it happens with benzene, toluene and the xylenes.

Reforming catalysts require the presence of two catalytic functions. One is the de/hydrogenating function, which is provided by noble metal particles. The other is the isomerization/cyclization function, which is provided by acid sites of the catalyst support. The first naphtha reforming catalysts appeared in 1949 [1,2]. These catalysts were made of Pt particles supported on alumina. The latter was chlorided in order to promote its acidity. In 1968 these catalysts were replaced by bimetallic catalysts of the Pt–Re/Al_2O_3–Cl type [3]. The new catalysts had a higher resistance to coke deactivation and a higher selectivity to aromatics and isoparaffins. They also enabled the process to be performed at a lower pressure.

The last improvements in the naphtha reforming technology have been aimed at increasing the length of the operation cycle and with this purpose new trimetallic catalysts have reached the market which are even more selective and resistant to coke deactivation than bimetallic catalysts. As it usually happens in the petrochemical industry, catalytic materials have been synthesized, optimized and put into operation, while still lacking a theory about the catalytic phenomena involved. Due to the economical importance of their technology, the process companies that license-reforming processes do not publish any data about the exact chemical composition and structure of their catalysts. As a consequence very scarce information is found in the open literature about trimetallic catalysts.

We have recently studied the influence of the order of addition of the metal precursors on the catalytic properties of

* Corresponding author. Tel.: +54 342 4533858; fax: +54 342 4692456.
E-mail address: pieck@fiqus.unl.edu.ar (C.L. Pieck).

0920-5861/$ – see front matter © 2005 Elsevier B.V. All rights reserved.
doi:10.1016/j.cattod.2005.07.042

trimetallic Pt–Re–Sn/Al_2O_3–Cl catalysts. These properties included: Pt resistance to sulfur poisoning, Pt metal activity and selectivity in hydrocarbon metal-catalyzed reforming reactions, amount and distribution of acid strength, activity and selectivity in acid-catalyzed reactions [4–6]. We are complementing these series of studies in this work by studying the influence of the Sn content on the catalytic activity and selectivity of trimetallic Pt–Re–Sn/Al_2O_3–Cl catalysts.

2. Experimental

2.1. Catalysts preparation

All catalysts were prepared using a commercial γ-alumina as support (Cyanamid Ketjen CK-300, pore volume = 0.5 $cm^3\ g^{-1}$, specific surface area = 180 $m^2\ g^{-1}$, impurities: Na = 5 ppm, Fe = 150 ppm, S = 50 ppm). The alumina pellets were ground to 35–80 meshes and then were calcined in air at 650 °C for 3 h. The Pt–Re/γ-alumina catalyst was prepared by means of coimpregnation of the Pt and Re salts followed by calcination in air (4 h, 500 °C) and reduction in hydrogen (4 h, 500 °C). Trimetallic catalysts were prepared by the method of coimpregnation. In all cases the impregnation volume was adjusted in order to yield the appropriate final concentration of each metal in the catalysts. The salts used (concentration of the impregnating aqueous solution between brackets) were: $H_2PtCl_6{\cdot}6H_2O$ (3.345 mg Pt cm^{-3}), $SnCl_2{\cdot}2H_2O$ (25 mg Sn cm^{-3}) and NH_4ReO_4 (20.18 mg Re cm^{-3}). The solution of the Sn precursor was unstable and was prepared just before its use. $SnCl_2$ was first dissolved in deionized water and heated for 30 min at 70 °C. Then aliquots of 37% HCl were added until the solution became transparent and was ready to be used. An amount of 0.2 M HCl solution was added to the support (1.5 $cm^3\ g^{-1}$) before impregnating the metal salts in order to add chloride as a competing ion and to assure a homogeneous distribution of them. The solution containing the catalyst was first left unstirred for 1 h and then was gently heated at 70 °C in order to evaporate the excess liquid. The catalysts were finally dried at 120 °C overnight, calcined in air (4 h, 500 °C) and reduced in hydrogen (4 h, 500 °C).

Each catalyst was given a name in which the metal names are separated with hyphens and the metal content is written between brackets, e.g. Pt–Re–Sn(0.1)/Al_2O_3. When not indicated the metal content is 0.3%, i.e. Pt–Re/Al_2O_3 is equivalent to Pt(0.3)–Re(0.3)/Al_2O_3.

2.2. Temperature programmed reduction

TPR tests were performed in an Ohkura TP2002 apparatus equipped with a thermal conductivity detector. At the beginning of each TPR test the sample was heated in air at 450 °C for 1 h. Then it was heated from room temperature to 700 °C at a heating rate of 10 °C min^{-1} in a reducing gas stream (5.0% H_2 in argon).

2.3. Temperature programmed pyridine desorption

The quantity and amount of acid sites on the catalysts surface was assessed by means of temperature programmed desorption of pyridine. Two hundred milligrams of the catalyst were first immersed in a closed vial containing pure pyridine (Merck, 99.9%) for 4 h. Then the catalyst was taken out from the vial and excess pyridine was removed by evaporation at room temperature under a fume hood. The sample was then charged to a quartz micro reactor and a constant nitrogen flow (40 $cm^3\ min^{-1}$) was set up. Weakly adsorbed pyridine was first desorbed in a first stage of stabilization by heating the sample at 110 °C for 2 h. The temperature of the oven was then raised to 600 °C at a heating rate of 10 °C min^{-1}. The reactor outlet was directly connected to a flame ionization detector to measure the desorption rate of pyridine.

2.4. CO chemisorption

The experiments were performed in a chemisorption equipment designed ad hoc. The catalyst was placed in a quartz reactor and firstly reduced in a hydrogen stream (500 °C, 2 h, 60 $cm^3\ min^{-1}$). Then the carrier gas was switched to N_2 and the adsorbed hydrogen was desorbed (500 °C, 60 $cm^3\ min^{-1}$) during 1 h and then the cell was cooled to room temperature. Then 0.25 cm^3 pulses of diluted CO (3.5% CO in N_2) were fed to the reactor. Non chemisorbed CO was quantitatively transformed into CH_4 over a Ni/Kieselgur catalyst and detected in a flame ionization detector connected on-line.

2.5. Temperature programmed oxidation

Carbon deposits forming on the surface of the catalysts were studied by means of temperature programmed oxidation (TPO). 40–60 mg of the coked catalyst were first charged in a quartz reactor. Then the carbon was burned in an oxidizing stream (60 $cm^3\ min^{-1}$ of diluted oxygen, 5% O_2 in N_2, v/v). The temperature of the cell was increased from 30 to 650 °C with a heating rate of 10 °C min^{-1}. The outlet gases were fed to a methanation reactor where CO_2 and CO were quantitatively transformed into CH_4 over a Ni catalyst in the presence of H_2. The CH_4 stream was connected to a flame ionization detector (FID) and the signal produced was continuously recorded in a computer. The carbon concentration of the catalysts was calculated from the area of the TPO trace (FID signal as a function of the temperature of the cell) by reference to calibration experiments performed with catalysts with known carbon contents.

2.6. Cyclohexane dehydrogenation

The reaction was performed in a glass reactor with the following conditions: catalyst mass = 100 mg, temperature = 300 °C, pressure = 0.1 MPa, H_2 = 80 $cm^3\ min^{-1}$, cyclohexane = 1.61 $cm^3\ h^{-1}$. Before the reaction was

started, the catalysts were treated in H_2 (80 cm^3 min^{-1}, 500 °C, 1 h). The reaction products were analyzed in a gas chromatograph connected on-line.

2.7. n-Pentane isomerization

It was carried out in a glass reactor, for 4 h, at 500 °C, 0.1 MPa, WHSV = 4.5 and molar ratio H_2:*n*-C_5 = 6. *n*-C_5 was supplied by Merck (99.9%). The analysis of the reaction products was performed in a gas chromatograph connected on-line. Before the reaction, the catalysts were reduced at 500 °C for 1 h with hydrogen.

2.8. n-Heptane dehydrocyclization

One hundred and fifty milligrams of the catalyst were charged to a glass reactor and the reaction was carried out for 6 h at 450 °C, H_2/*n*-C_7 = 4 and WHSV = 7.3. Before the reaction test the catalysts were reduced in hydrogen (500 °C, 1 h, 10 cm^3 min^{-1}). The reaction products were analyzed in a gas chromatograph connected on-line.

In the *n*-pentane, cyclohexane and *n*-heptane reactions the conditions ensured that they proceeded under chemical control with no mass transfer problems, as revealed by the calculus of the Weisz–Prater modulus ($\Phi \ll 0.01$) and the Damköhler number ($Da \approx 0$). The mass transport coefficients were estimated from known correlations.

3. Results and discussion

Fig. 1 shows the TPR traces of the monometallic catalysts. Pt/Al_2O_3 has a large hydrogen consumption peak centered at 250 °C. The total hydrogen consumption (TPR area) corresponds to the total reduction of Pt(IV) to Pt(0).

The TPR trace of Sn oxide is very broad, starting at 150 °C and ending at 550 °C, with two main reduction zones in the 200–300 and 380–520 °C ranges. This is an indication of an interaction between Sn oxide and alumina, probably producing tin aluminates. According to the literature [7] Sn(IV) is reduced to Sn(II) which, due to the strong interaction with the support, is not reduced to Sn(0). In our case, according to the hydrogen consumption, approximately 80% of Sn(IV) is reduced to Sn(II).

The TPR trace of Re oxide has a peak centered at about 580 °C with a small shoulder at a lower temperature that might correspond to the reduction of particles that because of their big size have a weak interaction with the support. The area under the peaks indicates that about 90% of Re oxide is reduced to metallic Re(0).

Fig. 2 shows the TPR plots of the Pt–Re/Al_2O_3 catalyst and the Pt–Re–Sn/Al_2O_3 catalysts. The bimetallic catalyst has two peaks, one at about 220 °C (attributed to Pt reduction) and the other at 360 °C (corresponding to Re reduction). It is noticeable the lower reduction temperature of Re in the bimetallic catalyst in comparison to monometallic Re/Al_2O_3. This effect has been reported by several researchers and it has been attributed to a catalytic reduction of Re by Pt [8,9].

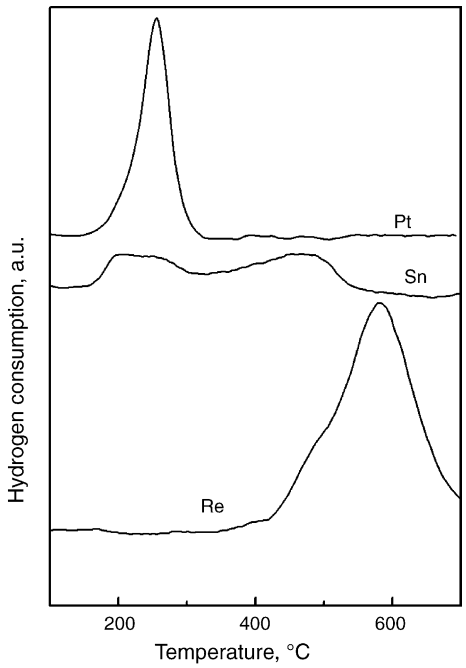

Fig. 1. Temperature programmed reduction (TPR) traces of monometallic catalysts.

As the Sn content was increased the temperature of the first reduction peak was shifted to higher temperatures. For Sn contents of 0–0.3% this effect seems to be due to the overlapping of the simultaneous reduction of Pt and Sn oxides that appear as a whole as a total shift to higher

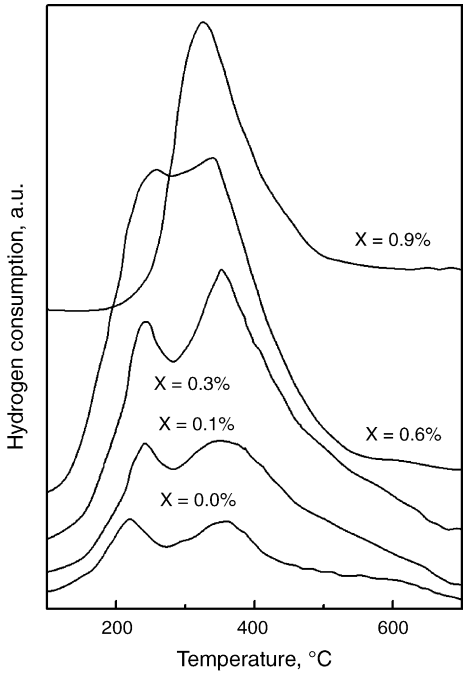

Fig. 2. TPR traces of trimetallic catalysts. *X*: Sn concentration.

temperatures. At 0.6% Sn the first and second peaks get closer and they finally get completely merged at 0.9% Sn. In this range of Sn concentration Pt, Re and Sn get in strong interaction probably because of the coimpregnation method used.

The amount of pyridine desorbed as a function of the heating temperature gives information on the total amount of acid sites and their strength distribution. Fig. 3 shows the influence of the Sn content on the total acidity and the distribution of acidity (weak, mild and strong acids sites) of the trimetallic catalysts. The distribution of acid sites was obtained by deconvolution of the pyridine TPD trace in three peaks. There is a rapid decrease of the total acidity upon addition of small amounts of Sn. Greater Sn amounts produce only a little additional acidity decreases. With respect to the acid distribution it can be seen that the Pt–Re catalyst has similar amounts of strong, mild and weak acid sites; the addition of Sn decreases more the population of weak and strong acid sites than the population of mild acid sites. In a previous work [5] we have reported that the catalyst with the greatest amount of acid sites is Pt and that the addition of Re or Sn decreases the total acidity. We have also reported that chlorided alumina has 40% more acid sites than the Pt monometallic catalyst. During impregnation, Cl is incorporated to γ-alumina and neutralizes all its basic sites. Cl is not an acid itself but it creates acid sites by polarizing the bonds of the Al cation. After surface water has been eliminated by calcination, Cl ions polarize the surface and produce approximately three acid sites per Cl atom. The amount of chlorine retained after calcination is practically the same for all catalysts (0.9%). The acidity decrease produced by addition of a metal (Pt, Re, Sn) can only be explained by the displacement of Cl atoms from Al sites where they generated acidity to other sites where they behave as spectators. Sn addition produces the neutralization of 10 acid sites per Sn atom, i.e. Sn on average inhibits three Cl atoms. In the case of Re and Pt, the competition with Cl anions for the surface adsorption sites of alumina produces a similar but less strong effect [5]. In the trimetallic catalysts the acidity stabilization at high Sn contents can be explained by considering that big amounts of Sn produce Sn particles of low dispersion that have a lower interaction with the support. It can be concluded that Sn not only decreases the total amount of acid sites but also changes their distribution; the strong and weak acid sites are the most affected ones.

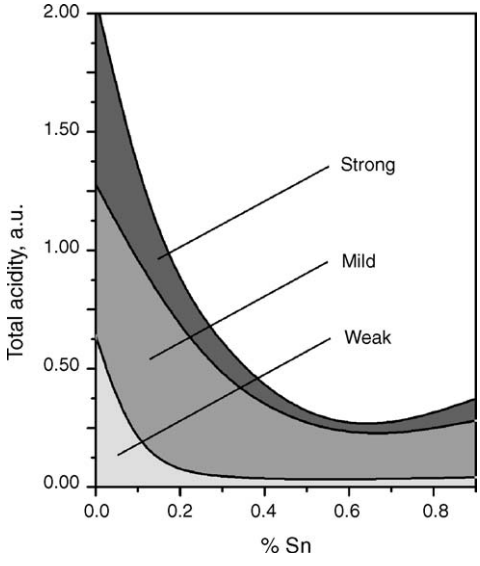

Fig. 3. Total acidity and acid strength distribution as obtained by temperature programmed desorption of pyridine. Trimetallic catalysts.

Fig. 4 shows the results obtained in the cyclohexane reaction tests and the CO chemisorption experiments. The Pt/Al_2O_3 catalyst was the most active in cyclohexane dehydrogenation, with an average conversion of 53.6%, while the Sn/Al_2O_3 and Re/Al_2O_3 catalysts had negligibly activity (not shown). The addition of Re produced a decrease in the activity of Pt/Al_2O_3. $Pt–Re/Al_2O_3$ had 45.8% conversion and the addition of growing amounts of Sn produced a proportional decrease of the conversion of cyclohexane. The activity loss is related to the inhibiting effect of Sn that either blocks the surface Pt atoms (geometry effect) or modifies the electronic properties of the active Pt atoms (electronic effect). As the Sn content increases the amount of chemisorbed CO decreases. There is a direct correlation between the activity for CH dehydrogenation and the amount of CO chemisorbed. These results show that it is possible to predict the metal activity of trimetallic Pt–Re–Sn/Al_2O_3 catalysts from CO chemisorption data.

Table 1 contains conversion values corresponding to the n-C_5 test reaction, along with values of the molar ratio C_1/C_3, the selectivity to i-C_5 isomers, and the percentage of carbon on the catalyst at the end of the run. The selectivity to

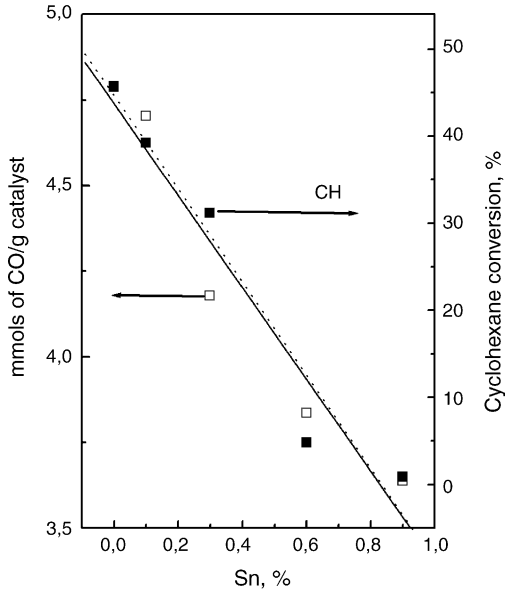

Fig. 4. CO chemisorption and cyclohexane conversion of trimetallic catalysts. Linear correlation of the cyclohexane dehydrogenation activity (dotted line) and the CO chemisorption capacity (solid line) as a function of Sn content.

Table 1
Conversion and selectivity values at the end of the *n*-pentane reaction test

Catalyst	Conversion (%)	Selectivity (%)			C_1/C_3 (M)	Carbon (%)
		i-C_5	C_1	C_3		
Pt/Al_2O_3	32.2	20.2	0.80	4.70	0.51	0.59
$Pt–Re/Al_2O_3$	20.1	23.1	2.11	9.50	0.67	0.34
$Pt–Re–Sn(0.1)/Al_2O_3$	42.4	48.4	0.45	5.90	0.23	0.49
$Pt–Re–Sn(0.3)/Al_2O_3$	38.1	40.7	0.17	2.90	0.18	0.43
$Pt–Re–Sn(0.6)/Al_2O_3$	37.0	35.9	0.16	2.80	0.17	0.35
$Pt–Re–Sn(0.9)/Al_2O_3$	24.5	30.4	0.13	2.30	0.17	0.31

Final carbon contents after the end of the run.

each product was calculated according to the following formula:

$$S_i = \frac{A_i \mathrm{rf}_i \mathrm{CN}_i \times 100}{X \sum A_i \mathrm{rf}_i \mathrm{CN}_i} \quad (1)$$

where X is the total conversion, A_i the chromatographic area of the ith compound, rf_i the response factor of the ith compound and CN_i is the carbon number of the ith compound.

Isoparaffins were the main reaction products and there was no formation of aromatic hydrocarbons. It is accepted that the isomerization of *n*-paraffins proceeds through a bifunctional metal–acid mechanism [10]. The reaction starts on the metal site with the dehydrogenation of the paraffin to an olefin. The olefin then moves to the acid site where it is converted to an alkene isomer. This alkene is finally hydrogenated on a metal site. The reaction mechanism is controlled by the slowest elemental step on the acid function [11]. Therefore the formation of isopentane can be taken as an indirect measure of the activity of the acid function. It has been reported that the isomerization of *n*-paraffins can also proceed by a monofunctional metal-catalyzed mechanism, by means of the hydrogenolysis of a ring of five carbon atoms [12–14]. However, the contribution of this reaction pathway is negligible in the reaction conditions of naphtha reforming [15].

It can be seen that the addition of Re to Pt/Al_2O_3 decreases the isomerization yield while the addition of Sn to Pt–Re increases it. This is a consequence of the control of the global isomerization reaction rate by the acid function reaction step. Shen et al. [16] have pointed out that the addition of Sn decreases the acidity of the support (as confirmed by our TPD results) and mainly the fraction of strong acid sites. Therefore, the hydrocracking occurring on the strong acid sites is inhibited. Conversely the fraction of sites of mild acid strength is increased; the isomerization is consequently enhanced, because it does not need acid sites of high strength [12,13]. With respect to the metal function, Sn addition also decreases the hydrogenolysis activity of Pt–Re. Therefore, there is an indirect increase of the isomerization products due to the inhibition of the cracking on the metal function. Hydrogenolysis is a demanding reaction and methane (C_1) a typical product [17].

In the case of the $Pt–Re/Al_2O_3$ catalyst there is a synergistic effect in the hydrogenolysis reaction. The magnitude of the heat of adsorption is decisive for the formation of the complex that leads to the cleavage of the C–C bond. An ensemble of Pt atoms has a small heat of adsorption, single Re atoms have a great value and Pt–Re ensembles have an intermediate value. For this reason a Pt–Re ensemble has a higher activity than Pt or Re individually [18,19]. One proof is the higher C_1/C_3 ratio found in the products of the reaction performed on the $Pt–Re/Al_2O_3$ catalyst, in comparison to the reaction catalyzed by Pt/Al_2O_3 or $Pt–Re–Sn/Al_2O_3$. The lower production of *i*-C_5 in the case of the $Pt–Re/Al_2O_3$ catalyst might therefore be due to the destruction of the intermediate isoolefins by hydrogenolysis on the metal function.

With respect to the formation of coke it can be seen that both the addition of Re and the addition of Sn decrease the coke yield in comparison to the monometallic Pt/Al_2O_3 catalyst. These results must be related to the different acid strength of the catalysts and the different metal activity. Coke formation is a complex phenomenon; the metal produces coke precursors by dehydrogenation [20] and also destroys them by hydrogenolysis [21]. The metal also participates in the stabilization of the coke deposits on the support because it activates the elimination of adsorbed hydrogen by inverse spillover [21]. The acid function is responsible for the accumulation of coke because it polymerizes the unsaturated coke precursors [22].

When Sn is added to the Pt–Re catalyst, there is an important improvement of the catalytic activity (conversion) even when small amounts are used. Too high Sn loadings produce a decrease of the catalytic activity. The beneficial effect of Sn addition can be seen both in the improvement of the isomerization activity and in the lowering of the C_1/C_3 ratio which is a comparison of the hydrogenolytic activity on the metallic function (producing C_1) and the cracking activity on the acid function (producing C_3). With respect to the coking, all $Pt–Re–Sn/Al_2O_3$ catalysts, with the sole exception of the 0.9% one, have greater carbon deposits than the $Pt–Re/Al_2O_3$ catalyst. In spite of these bigger carbon deposits, $Pt–Re–Sn/Al_2O_3$ catalysts are more active and have a higher selectivity to C_5 isomers. This is not contradictory because the coke on Pt–Re–Sn might be mostly on strong acid sites.

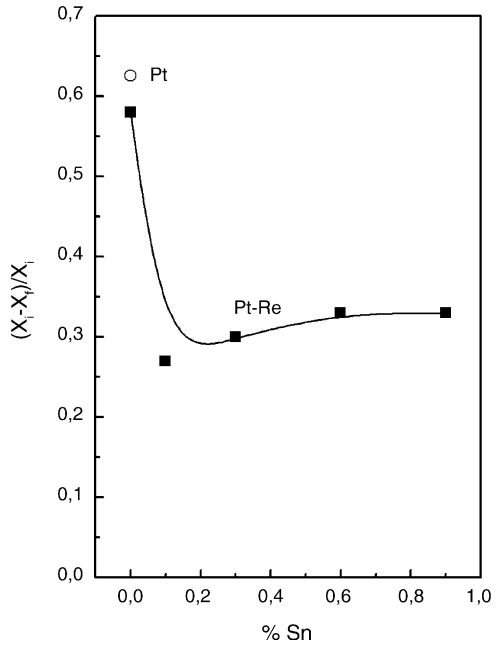

Fig. 5. *n*-Pentane reaction. Pt–Re–Sn/Al_2O_3 catalysts. [(Initial conversion − final conversion)/initial conversion] as a function of the Sn content.

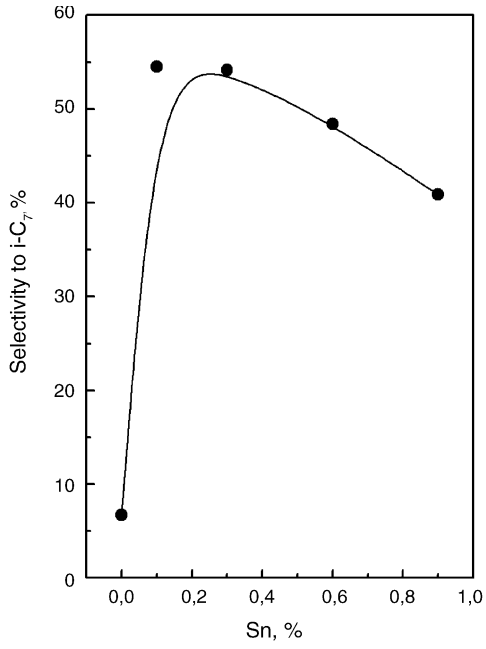

Fig. 6. *n*-Heptane reaction. Pt–Re–Sn/Al_2O_3 catalysts. Selectivity to *i*-C_7 as a function of the Sn content, 240 min time-on-stream. Value for Pt/Al_2O_3: *i*-C_7 = 36.64%.

Fig. 5 is a plot that shows the deactivation in the runs with *n*-pentane. It shows the values of χ = [(initial conversion − final conversion)/initial conversion] as a function of the Sn content of the Pt–Re–Sn catalysts. χ is related to the stability of the catalysts being lower for stable catalysts. The χ value of Pt was also included in order to make a comparison. A great improvement in stability is found upon addition of even small quantities of Sn; big coke deposits on Pt–Re–Sn do not translate into low χ values. This fact can be explained by supposing that there are coke deposits of different toxicity, and that this toxicity is a function of the properties of the catalysts [23].

Table 2 shows the conversion values obtained at 5 and 240 min of time-on-stream during the *n*-C_7 reaction tests. It can be seen that the addition of Re to Pt/Al_2O_3 improves the activity and stability. The addition of Sn to bimetallic Pt–Re/Al_2O_3 decreases the initial activity (5 min time-on-stream) due to the combined effects of decrease of acidity and hindering of metal accessibility. The stability is increased at low Sn contents. Values of selectivity to aromatic hydrocarbons are also included in Table 2. The selectivity to each product was calculated according to Eq. (1).

The addition of Re to the Pt/Al_2O_3 catalyst decreases the formation of aromatic compounds. The addition of Sn to the Pt–Re/Al_2O_3 catalyst produces an increase at low Sn concentrations (0.1 and 0.3%) and a decrease at higher concentrations (0.6 and 0.9%). Aromatic hydrocarbons are produced by dehydrocyclization of paraffins, a reaction that occurs mainly by a bifunctional mechanism under the reforming conditions [15]. The paraffins are first dehydrogenated on the metal to give *n*-olefins, which migrate to a neighboring acid site, where they are protonated, producing a secondary carbenium ion. This ion is cycled on the acid function, producing five-carbon-atom ring olefins, which are then isomerized on the acid sites, enlarging the ring to six carbons. In this way cyclohexene and cyclohexadiene (with and without branches) are dehydrogenated to aromatic hydrocarbons. The dehydrogenation–hydrogenation reac-

Table 2
Conversion and selectivity to aromatics and to ($C_1 + C_2 + C_3$)

Catalyst	Conversion (%)		Selectivity (%)			
	5 min	240 min	Aromatics		$C_1 + C_2 + C_3$	
			5 min	240 min	5 min	240 min
Pt/Al_2O_3	55.26	21.78	34.47	16.65	5.80	4.48
Pt–Re/Al_2O_3	57.62	27.66	18.87	4.40	11.33	7.61
Pt–Re–Sn(0.1)/Al_2O_3	52.19	41.50	36.30	20.60	10.14	6.50
Pt–Re–Sn(0.3)/Al_2O_3	50.99	38.72	30.07	16.49	7.84	7.68
Pt–Re–Sn(0.6)/Al_2O_3	35.05	30.00	12.80	13.00	6.90	5.50
Pt–Re–Sn(0.9)/Al_2O_3	14.18	10.46	5.96	6.19	4.77	4.49

n-Heptane reaction test, 5 min, 240 min time-on-stream.

tions on the metal function are rapid enough to be considered in thermodynamic equilibrium, whereas isomerization reactions on the acid function are slower [15]. Therefore the highest selectivity to aromatic compounds is expected to take place on the most acidic catalysts. The acidity values obtained directly by pyridine TPD or indirectly by analyzing the selectivity to i-C_5 in the n-C_5 reaction test, show that the trimetallic catalyst with the highest acid strength is Pt–Re–Sn(0.1). This catalyst also has the best selectivity to aromatic compounds.

The yields to $(C_1 + C_2 + C_3)$ hydrocarbons decrease monotonically as the Sn content is increased, in accord with the acidity decrease. It must be remembered that hydrocracking to light products occurs over strong acid sites and that the pyridine TPD results confirm that the amount of strong acid sites decreases with Sn addition.

Fig. 6 shows the selectivity to C_7 isomers at the end of the run (240 min time-on-stream) as a function of the Sn content. All trimetallic catalysts are more selective for the production of i-C_7 than Pt–Re/Al_2O_3 but the selectivity decreases as the Sn content increases. The shape of the curve is the result of both isomerization and hydrocracking acting together. Isomerization proceeds by a bifunctional mechanism and the global reaction rate is controlled by the skeletal isomerization on the acid sites, therefore the isomerization activity always decreases upon Sn addition. Hydrocracking is also catalyzed by the acid function [15]. Paraffins are first cracked in the middle, resulting in low methane production. The products are not further cracked within certain contact times, but at high conversion and residence time values, successive or secondary hydrocracking increase the yield of lower paraffins. The increase of the i-C_7 selectivity upon addition of small amounts of Sn must therefore be due to the inhibition of hydrocracking. It must be remembered that Sn addition mainly decreases the population of strong acid sites. The subsequent decrease upon addition of greater amounts of Sn must be due to the decrease of the isomerization rate.

Fig. 7 shows the C_1/C_3 ratio at 5 and 240 min of time-on-stream as a function of the Sn content. This ratio is a comparison of the hydrogenolytic activity of the metal function and the cracking activity of the acid function. It is accepted that C_1 is produced on the metal surface by hydrogenolysis [17], a demanding reaction [24], while C_3 is produced on acid sites by hydrocracking. Our results are in accord with those of Agustine and Sachtler [18,19] who found that the formation of C_1 is higher on Pt–Re/Al_2O_3 than on Pt/Al_2O_3. The addition of Sn destroys Pt–Re ensembles and inhibits the hydrogenolysis activity [25,26]. From the values of the C_1/C_3 ratio, it is clear that Sn addition affects more the metal function than the acid function. For comparison the C_1/C_3 values of Pt/Al_2O_3 are included as a footnote to Fig. 7.

Fig. 8 shows the benzene/i-C_7 ratio obtained at 240 min of time-on-stream as a function of the Sn content of trimetallic catalysts. The addition of 0.10% Sn to Pt–Re decreases almost three times the benzene/i-C_7 ratio. At higher Sn contents the decrease is a little higher. This effect could be related to a decrease of the hydrogenolytic activity of the metal and therefore a decrease of the benzene coming from toluene dealkylation. Fig. 9 also shows that the aromatics/i-C_7 ratio slowly decreases with Sn content. Dehydrocyclization and isomerization reactions are both controlled by the acid function and are therefore inhibited because the amount and strength of the acid sites are

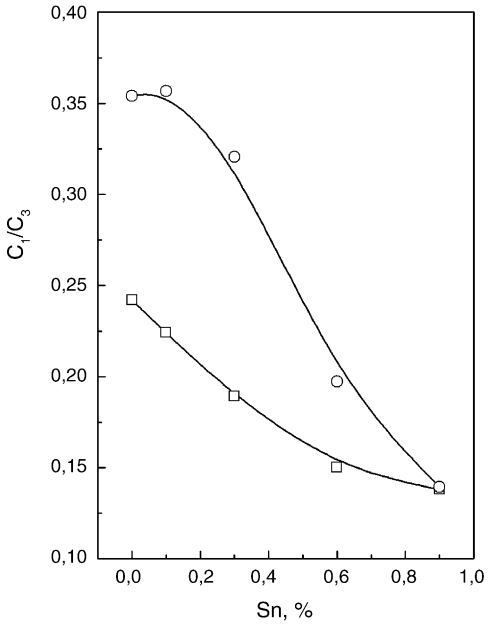

Fig. 7. n-Heptane reaction. C_1/C_3 molar ratio as a function of the Sn content. Pt–Re–Sn/Al_2O_3 catalysts. (○) Initial (5 min time-on-stream), (□) final (240 min time-on-stream). Values for Pt/Al_2O_3: initial, 0.254; final, 0.129.

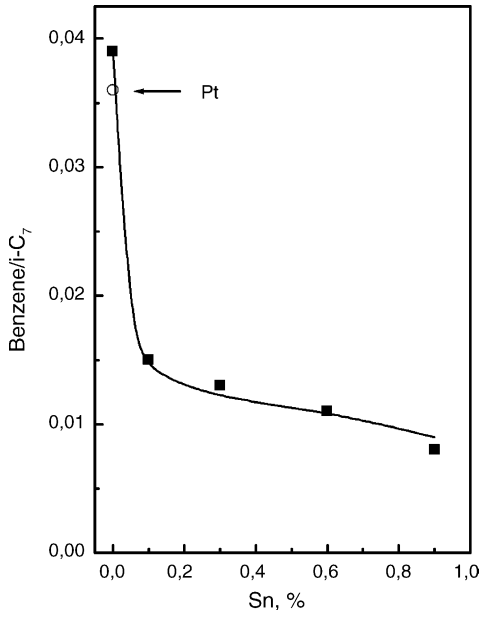

Fig. 8. n-Heptane reaction. Benzene/i-C_7 isomers molar ratio as a function of the Sn content. Pt–Re–Sn/Al_2O_3 catalysts at 240 min time-on-stream.

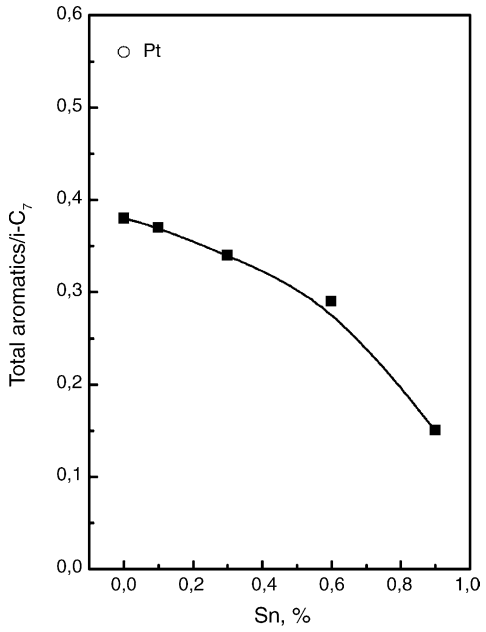

Fig. 9. *n*-Heptane reaction. Total aromatics/*i*-C_7 isomers molar ratio as a function of the Sn content. Pt–Re–Sn/Al_2O_3 catalysts at 240 min time-on-stream.

decreased by Sn addition. The Pt–Re–Sn(0.1)/Al_2O_3 catalyst produces more aromatic compounds, more *i*-C_7 isomers and less benzene than Pt–Re/Al_2O_3. These results are a combined effect of the lower hydrogenolytic activity and the lower cracking activity, which are a result of a better acid strength distribution and the blocking of Pt–Re ensembles.

4. Conclusions

In Pt(0.3)–Re(0.3)–Sn(*X*)/Al_2O_3 trimetallic catalysts the acidity is decreased as the Sn load is increased. Weak and strong acids sites are the most affected acid sites. Eventually a point is reached in which further Sn addition does not decrease the acidity probably because of the formation of Sn species of low dispersion.

The results of the *n*-C_5 and *n*-C_7 test reactions show that the addition of Sn to the Pt–Re/Al_2O_3 catalysts, especially in small amounts, greatly improves the stability, activity and selectivity of the catalyst. The addition of Sn to the Pt–Re catalyst decreases the benzene/*i*-C_7 ratio yielding product streams with lower environmental impact.

References

[1] V. Hansel, U.S. Patent 2,479,101 (1949) UOP.
[2] V. Hansel, U.S. Patent 2,479,110 (1949) UOP.
[3] H.E. Klusksdahl, U.S. Patent 3,415,737 (1968) Chevron.
[4] L.S. Carvalho, C.L. Pieck, M.C. Rangel, N.S. Fígoli, J.M. Grau, P. Reyes, J.M. Parera, Appl. Catal. A 269 (2004) 91.
[5] L.S. Carvalho, C.L. Pieck, M.C. Rangel, N.S. Fígoli, C.R. Vera, J.M. Parera, Appl. Catal. A 269 (2004) 105.
[6] L.S. Carvalho, C.L. Pieck, M.C. Rangel, N.S. Fígoli, J.M. Parera, Ind. Eng. Chem. Res. 43 (2004) 1222.
[7] R. Bacaud, P. Bussiere, F. Figueras, M. Mathieu, CR Acad. Sci. Paris Ser. C 281 (1975) 159.
[8] B.H. Isaac, E.E. Petersen, J. Catal. 85 (1984) 8.
[9] L. Chen, Y. Li, J. Zang, H. Luo, S. Cheng, J. Catal. 145 (1994) 132.
[10] G.A. Mills, H. Heinemann, T.H. Milleken, A.G. Oblad, Ind. Eng. Chem. 45 (1953) 134.
[11] C.A. Querini, N.S. Fígoli, J.M. Parera, Appl. Catal. 52 (1989) 249.
[12] D.E. Sparks, R. Srinivasan, B.H. Davis, J. Mol. Catal. 88 (1994) 325.
[13] D.E. Sparks, R. Srinivasan, B.H. Davis, J. Mol. Catal. 88 (1994) 359.
[14] R. Srinivasan, B.H. Davis, J. Mol. Catal. 88 (1994) 343.
[15] J.M. Parera, N.S. Fígoli, in: G.J. Antos, A.M. Aitani, J.M. Parera (Eds.), Catalytic Naphtha Reforming: Science and Technology, Marcel Dekker Inc., New York, 1995 (Chapter 3).
[16] J. Shen, R.D. Cartright, Y. Chen, J.A. Dumesic, Catal. Lett. 26 (1994) 247.
[17] J.H. Sinfelt, J. Catal. 29 (1973) 308.
[18] S.M. Agustine, W.M.H. Sachtler, J. Catal. 106 (1987) 417.
[19] S.M. Agustine, W.M.H. Sachtler, J. Phys. Chem. 91 (1987) 5753.
[20] C.L. Pieck, P. Marécot, J.M. Parera, J. Barbier, Appl. Catal. A: Gen. 126 (1995) 153.
[21] J. Barbier, in: B. Delmon, G.F. Froment (Eds.), Catalyst Deactivation, Elsevier, Amsterdam, 1987, p. 1.
[22] B.J. Cooper, D.L. Trinn, in: B. Delmon, G.F. Froment (Eds.), Catalyst Deactivation, Elsevier, Amsterdam, 1980, p. 63.
[23] C.L. Pieck, P. Marécot, J. Barbier, Appl. Catal. A 145 (1996) 323.
[24] M. Boudart, A. Aldag, J.E. Benson, N.A. Dougharty, C.G. Harkins, J. Catal. 6 (1966) 92.
[25] F.M. Dautzenberg, J.N. Helle, P. Biloen, W.M.H. Sachtler, J. Catal. 63 (1980) 119.
[26] R.D. Cartright, J.A. Dumesic, J. Catal. 148 (1994) 771.